Vacuum 85 (2010) 358–364

Contents lists available at ScienceDirect

Vacuum

journal homepage: www.elsevier.com/locate/vacuum

Influence of Se on the electron mobility in thermal evaporated $Bi_2(Te_{1-x}Se_x)_3$ thin films

L.I. Soliman [a,*], M.M. Nassary [b], H.T. Shaban [b], A.S. Salwa [b]

[a] National Research Centre, Solid State Physics Department, Cairo, Egypt
[b] South Valley University, Qena, Faculty of Science, Egypt

ARTICLE INFO

Article history:
Received 16 August 2009
Received in revised form
8 June 2010
Accepted 15 June 2010

Keywords:
Thermoelectric materials $Bi_2(Te_{1-x}Se_x)_3$
Thin films
Electrical properties

ABSTRACT

Thermoelectric solid solutions of $Bi_2(Te_{1-x}Se_x)_3$ with $x = 0$, 0.2, 0.4, 0.6, 0.8 and 1 were grown using the Bridgman technique. Thin films of these materials of different compositions were prepared by conventional thermal evaporation of the prepared bulk materials. The temperature dependence of the electrical conductivity σ, free carriers concentration n, mobility μ_H, and seebeck coefficient S, of the as-deposited and films annealed at different temperatures, have been studied at temperature ranging from 300 to 500 K. The temperature dependence of σ revealed an intrinsic conduction mechanism above 400 K, while for temperatures less than 400 K an extrinsic conduction is dominant.

The activation energy, ΔE, and the energy gap, E_g, were found to increase with increasing Se content. The variation of S with temperature revealed that the samples with different compositions x are degenerate semiconductors with n-type conduction. Both, the annealing and composition effects on Hall constant, R_H, density of electron carriers, n, Hall mobility, μ_H, and the effective mass, m^*/m_0 are studied in the above temperature range.

1. Introduction

Thermoelectric materials and cells have attracted considerable interest due to the requirement of environment protection and other applications. Bismuth telluride and its derivative selenium compounds are considered to be the best materials for the use in thermoelectric devices near room temperature. The thermoelectric devices are used by the military for night vision equipment, electronic equipment cooling, portable refrigerators, and internal guidance systems [1]. Bi_2Te_3, Bi_2Se_3 and their solid solution crystals are narrow-band-gap semiconductors with asymmetric band structure, they have rhombohedral unit cell with symmetric space group D_3^5 (R3m) [2]. Optical band gap energies for Bi_2Te_3 and Bi_2Se_3 have values ranging from 0.13 to 1.4 eV and from 0.12 to 2.35 eV [3–5] respectively. The alloy system of Bi_2Te_3–Bi_2Se_3 has energy band gap ranging from 0.2 to 0.3 eV [6,8]. These attributes will impose some restrictions on the characterization of electrical properties such as Hall coefficient, carrier mobility and band gap energy of the Bi_2Te_3-based alloys. Thus most investigation on these alloys have been focused in order to tailoring their properties and to increase the thermoelectric conversion efficiency [9–18].

In order to achieve optimized properties of the thermoelectric materials, carrier concentration should be optimal and a ternary compound must be provided, switching from donor to acceptor and vice versa [19].

Even though a large volume of work has been done on the thermoelectric and optical properties of Bi_2Te_3 and Bi_2Se_3, they are not well defined, highly composition dependent, and not as efficient as the device needs to be. Hence, to improve the thermoelectric properties of these compounds, we try to change the Se contents x in the system $Bi_2(Te_{1-x}Se_x)_3$ thin films.

Most recently, Kim et al. and Carle et al. [20,21] reported the transport properties of $Bi_2(Te_{1-x}Se_x)_3$ thin films (x less than 0.05), and they found that, the composition and the thermal annealing affect these properties. The preparation and structural studies of the ternary compounds $Bi_2(Te_{1-x}Se_x)_3$ thin films were reported by the same authors [22].

The purpose of the present study is to report the electrical conductivity, thermoelectric power and Hall coefficient of polycrystalline $Bi_2(Te_{1-x}Se_x)_3$ thin films with $x = 0$, 0.2, 0.4, 0.6, 0.8, 1 prepared by conventional thermal evaporation technique as a function of temperature. Also, the effect of composition as well as the thermal annealing on the transport properties was studied.

* Corresponding author.
E-mail address: lailasoliman2000@yahoo.com (L.I. Soliman).

0042-207X/$ – see front matter © 2010 Elsevier Ltd. All rights reserved.
doi:10.1016/j.vacuum.2010.06.003

2. Experimental technique

The n-type nearly stoichiometric single-phase polycrystalline bulk ingot materials of $Bi_2(Te_{1-x}Se_x)_3$ with $x = 0$, 0.2, 0.4, 0.6, 0.8, 1 were synthesized by the modified Bridge man method [22] using the pure (99.999%) Te, Se, Bi elements contained in vacuum-sealed silica tubes ($\approx 1.5 \times 10^{-4}$ Pa), which have a constricted sharp end at the bottom to facilitate seeding in the growth process. In this method, the silica tube was held in the hot zone of the furnace about 24 h for complete melt of the composition. Then the tube was shaking during heating several times for homogenization. The rate of propagation of the crystallization front was 1.7 mm/h. The temperature of the middle zone ranges from 870 K to 995 K corresponding to the crystallization temperature of the prepared samples with different compositions. The duration time for producing the compound as crystal is about twelve days. The product crystal was 1.5 cm diameter and 1.5 cm in length.

Thin films were deposited by conventional thermal evaporation of the synthesized solid solutions onto Corning glass substrates held at room temperature, in vacuum of 10^{-4} Pa, using a high vacuum coating unit (Edwards 306 A). The deposition rate was kept constant during the evaporation process at nearly 3 nm/s. The film thickness was monitored using a quartz crystal thickness monitor (Edwards FTM4) and it was also measured interferometrically [23].

To anneal the thin films, they were slowly heated to different annealing temperatures 373, 423 and 473 K at a pressure of about 1.5×10^{-1} Pa, and kept at each annealing temperature for two hours. After annealing the films were allowed to cool slowly to room temperature in vacuum. The films annealed at $T \geq 423$ K were polycrystalline with single-phase of rhombohedral structure as that of bulk materials [22].

Electrical resistivity ρ was measured by the conventional four-probe method using a direct current. Thermoelectric power was determined by the constant temperature gradient method, using copper contacts under a temperature gradient of ≈ 10 K along the sample length. The Hall voltage was measured potentiometrically with usual precautions of reversing both the magnetic field and current. Moreover, the Hall voltage was taken as the average values when applying a magnetic field of 1 tesla at different current intensities.

The electrical conductivity σ, the thermoelectric power S, and the Hall voltage V_H were measured simultaneously on the same sample over the temperature range between 300 and 500 K. Thermoelectric power factor ($p = s^2\sigma$) was obtained from the seebeck coefficient and electrical conductivity.

3. Result and discussion

The composition as well as the crystal structure properties of $Bi_2(Te_{1-x}Se_x)_3$ ($x = 0$, 0.2, 0.4, 0.6, 0.8, 1) for both bulk and thin films were studied by the same authors [23]. They reported that, the Energy dispersive X-ray analysis (EDAX) of the investigated samples show that they are nearly stoichiometric with Bi deficiency of about 5% (Table 1). Also, X-ray diffraction analysis (XRD) of these samples confirmed that the bulk materials as well as the films annealed at temperatures 423 and 473 K, with different compositions are polycrystalline having rhombohedral structure. Whereas, the as-deposited and films annealed at 373 K are partially crystalline and have the same rhombohedral structure of the prepared bulk materials. Fig. 1 shows XRD of the annealed samples at 473 K for different compositions.

Table 1
Initially included and actually existing, using EDAX wt % of $Bi_2(Te_{1-x}Se_x)_3$ solid solutions.

Composition	Actual wt% calculated			Experimental wt%		
	Bi	Te	Se	Bi	Te	Se
Bi_2Te_3	40	60	–	40.77	59.23	–
$Bi_2Te_{2.4}Se_{0.6}$	40	48	12	40.93	49.23	9.84
$Bi_2Te_{1.8}Se_{1.2}$	40	36	24	38.22	36.64	25.14
$Bi_2Te_{1.2}Se_{1.8}$	40	24	36	37.52	28.34	34.14
$Bi_2Te_{0.6}Se_{2.4}$	40	12	48	36.76	13.87	49.37
Bi_2Se_3	40		60	39.97	–	60.03

3.1. Electrical conductivity

Conductivity is important and reliable information about the transport phenomena and other physical properties of the materials.

Fig. 2 shows the temperature dependence of the electrical conductivity of Bi_2Te_3, $Bi_2Te_{2.4}Se_{0.6}$, $Bi_2Te_{1.8}Se_{0.1.2}$, $Bi_2Te_{1.2}Se_{1.8}$, $Bi_2Te_{0.6}Se_{2.4}$, Bi_2Se_3 thin films of thickness 230 nm annealed at 473 K for two hour under vacuum. It is clear from Fig. 2 that, the electrical conductivity of all samples under investigation increases exponentially over the whole temperature range indicating normal semiconductor behaviour, which fits the relation:

$$\sigma = \sigma_0 \exp(-\Delta E/KT) \quad (1)$$

where σ_0 and ΔE represent the pre-exponential value and the activation energy respectively, and K is Boltzmann's constant.

The linear variation of $\log(\sigma)$ with $1/T$ indicated that the conduction in these samples is through thermally activated process, which agrees well with the results of other workers for polycrystalline chalcogenide materials [24,25]. This behaviour is expected given the rather low value of the energy gap in these semiconductor materials.

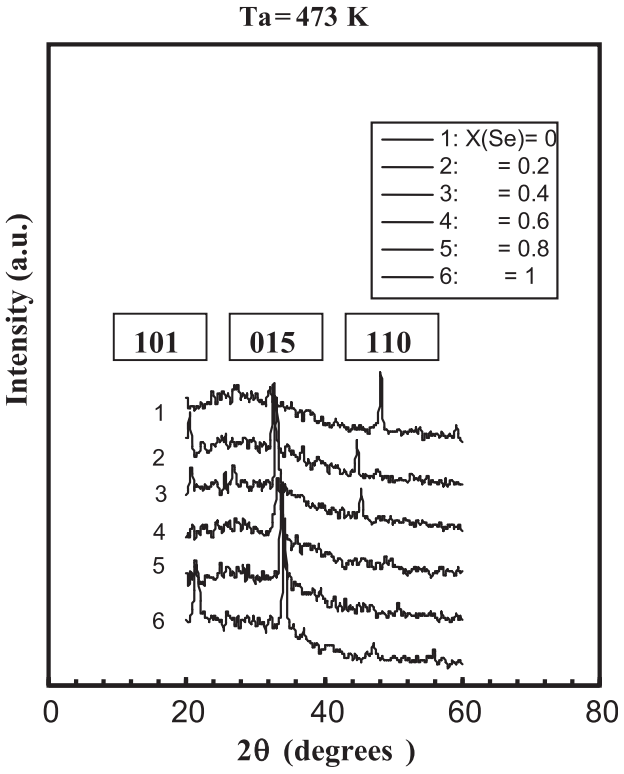

Fig. 1. X-ray diffraction patterns of $Bi_2(Se_xTe_{1-x})_3$ thin films annealed at $T_a = 473$ K.

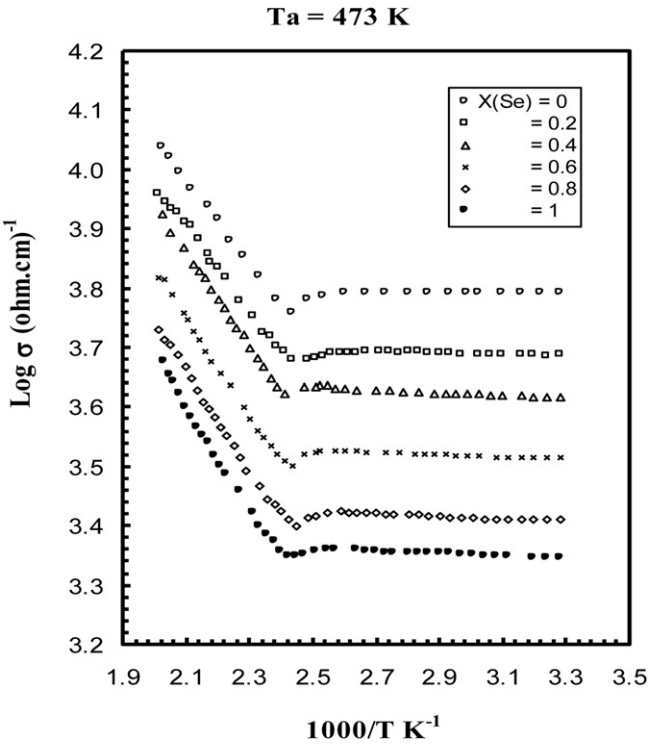

Fig. 2. The reciprocal temperature dependence of electrical conductivity $\log \sigma$ for $Bi_2(Se_xTe_{1-x})_3$ thin films annealed at 473 K.

The measured electrical conductivity for each composition indicated two straight lines with different slopes both fit relation (1). The first line corresponding to the low temperature range 300–400 K while the other line corresponding to the high temperature range 400–500 K indicating a transition occurs near 400 K. The activation energies ΔE_1 and ΔE_2 have been calculated using the slope of the two lines (Fig. 2).

In the temperature range 300–400 K, the values of ΔE_1 were found to increase from 0.003 to 0.0041 eV as x increases from 0 to1. Whereas, the activation energy, ΔE_2, in the temperature range 400–500 K was found to be half the optical energy gap, which was obtained previously by the same authors [26], indicating that the conduction mechanism in $Bi_2(Te_{1-x}Se_x)_3$ thin films at this temperature range is intrinsic whereas extrinsic conduction dominates in the low temperature range 300–400 K. The calculated electrical energy gap together with the activation energy for the samples is given in Table 2.

Moreover, both the activation energy, ΔE_1, and the electrical energy gap, E_g ($=2\Delta E_2$), were found to increase with composition x, as shown in Fig. 3

It can be seen that the evaluated thermal energy gaps are very close to those evaluated optically. This suggests the validity of the experimental measurements. Also, our results are close to the results published by Austin et al. [6] and Greenway et al. [7] for $Bi_2(Te_{1-x}Se_x)_3$ thin films where $x < 0.15$. The estimated optical energy gaps are ranged from 0.2 to 0.3 eV which are close to our experimental values.

Also, we noted that the transition from the extrinsic towards the intrinsic region happens at nearly the same temperature ($\approx$400 K) and is not concentration dependent.

Moreover, it is evident that increasing the selenium will lead to a decrease in the conductivity (Fig. 2) and an increase in the activation energy (Fig. 3) for all compositions. This may be attributed to enhanced valence band tailing with incorporation of selenium and the different value of the electro-negativity as well as the lattice

Table 2
The energy gap and activation energy data calculated from electrical measurements.

X(Se)	T_a (K)	$E_g(\sigma)$ (eV)	$\Delta E(\sigma)$ (eV)	$Eg(n)$ (eV)	$\Delta E(n)$ (eV)
		416–500 K	300–416 K	416–500 K	300–416 K
0	423	0.275	–	0.275	–
	473	0.273	–	0.273	–
0.2	423	0.28	0.0035	0.28	0.0035
	473	0.277	0.003	0.277	0.0031
0.4	423	0.314	0.004	0.313	0.0039
	473	0.31	0.0039	0.31	0.0038
0.6	423	0.319	0.004	0.319	0.004
	473	0.316	0.0039	0.316	0.0039
0.8	423	0.322	0.0042	0.323	0.0042
	473	0.32	0.004	0.32	0.004
1	423	0.333	0.0043	0.333	0.0043
	473	0.33	0.0041	0.331	0.0041

parameters for both Te and Se atoms. Also, at any given Se content, the electrical conductivity increases by increasing annealing temperature (see Fig. 4).

It is found also that our results of all samples are in good agreement with the XRD data and the Hall-effect measurements as will be shown below. Moreover, such behaviour is expected because of the low value of the energy gap ($\approx$0.3 eV) in these degeneracy semiconductor materials ($n \approx 10^{19}$ cm^{-3}).

A comparison of the present work for ternary materials could not be made since there are no reports on the electrical properties of bulk or thin films for these compositions. On the other hand our results of the electrical properties for samples with composition $x = 0$ and $x = 1$ agree well with reported results [27,28].

3.2. Hall effect

The Hall constants R_H were determined from the average measured values of the Hall voltage V_H in V using the well known relation:

$$R_H = \left(V_H t \times 10^4\right) \Big/ (I \cdot H) \qquad (2)$$

where I is the current in A passing through the sample, t is the thickness of the film in cm and H is the magnetic field strength in Tesla. The obtained values of R_H for the as-deposited $Bi_2(Te_{1-x}Se_x)_3$ thin films ($x = 0$, 0.2, 0.4, 0.6, 0.8 and 1), and those annealed at different annealing temperatures, indicated that all samples are

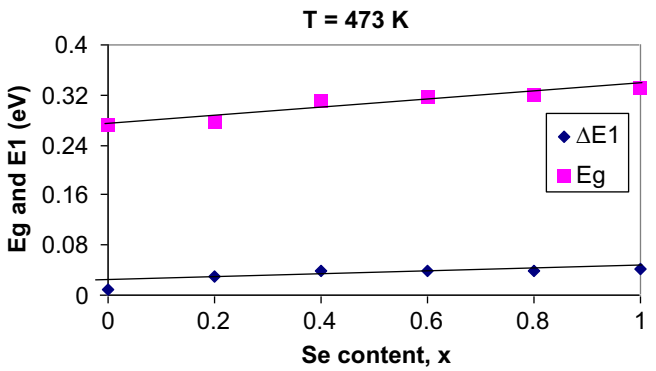

Fig. 3. compositional dependence of 1 – electrical energy gap E_g and 2 – thermal activation energy (ΔE_1) for $Bi_2(Se_xTe_{1-x})_3$ thin films annealed at 473 K.

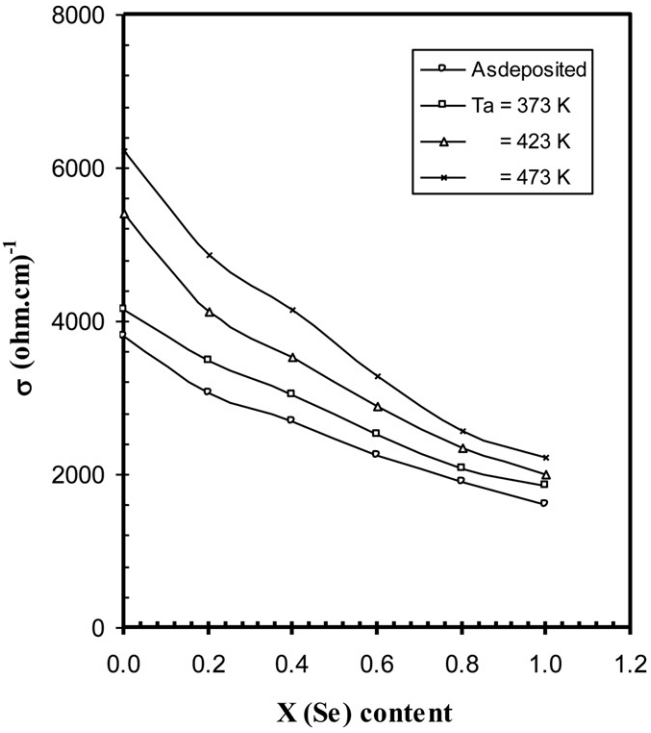

Fig. 4. Variation of d.c conductivity σ with composition x for the as-deposited (300 K) and annealed $Bi_2(Te_{1-x}Se_x)_3$ thin films.

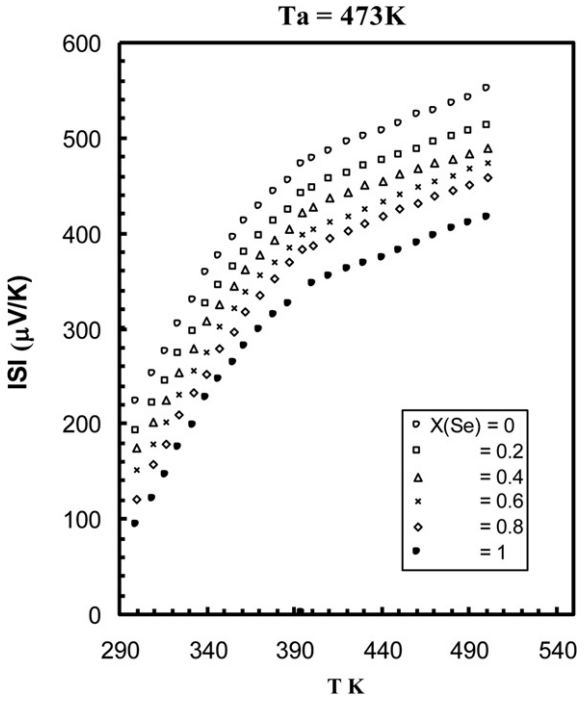

Fig. 5. Temperature dependence of Seebeck coefficient, S for $Bi_2(Se_xTe_{1-x})_3$ thin films annealed at 473 K.

n-type and R_H increases with increasing Se contents and decreases by increasing annealing temperature.

Also, a decrease in the absolute value of the Hall coefficient R_H is observed with increasing temperature, however, we can see that, at low temperature R_H is roughly constant, at temperature less than 400 K, This refers to the extrinsic behaviour of these semiconductors. The same behaviour has been observed from n-type Bi_2Te_3 [29].

3.3. Thermoelectric power

Thermoelectric properties of $Bi_2(Te_{1-x}Se_x)_3$ ($x = 0$, 0.2, 0.4, 0.6, 0.8, 1) films were measured from 300 K to 500 K. Fig. 5 illustrates the variation of the seebeck coefficient S with temperature for annealed films 473 K of the investigated samples. All the seebeck coefficients, S, are negative, which confirmed n-type conductivity of the films over the whole investigated temperature range i.e. the most predominant carriers are electrons which agree with Hall-effect measurements and this may be due to the deficiency of Bi and the excess of Te and Se as shown by EDAX. It is also seen that, the seebeck coefficient increases sharply with increasing the temperature at the range 300–400 K (extrinsic range) which indicated the degeneracy nature of the materials while shows a slow increase with temperature at the range 400–500 K for all samples. This behaviour may be due to the generation of the electrons from the valence band to the conduction band. Moreover, the value of seebeck coefficient S, decreases as Se contents increase, while, S increases with increasing annealing temperature as shown in Fig. 6.

The difference in the thermoelectric power of different compositions could be attributed to the effective mass value of each one.

Few authors reported the thermoelectric power for these materials with other compositions [6,7,24–26] and the values of (S) are very close to our reported one for Bi_2Te_3 and Bi_2Se_3 [27,28]. To confirm this behaviour of the thermoelectric power more detailed studies on the investigated samples are needed, as there is no reported data on these compositions.

The thermoelectric power factor P is commonly used to evaluate the performance of thermoelectric materials, especially for thin films, as a kind of figure of merit and it can be easily obtained from

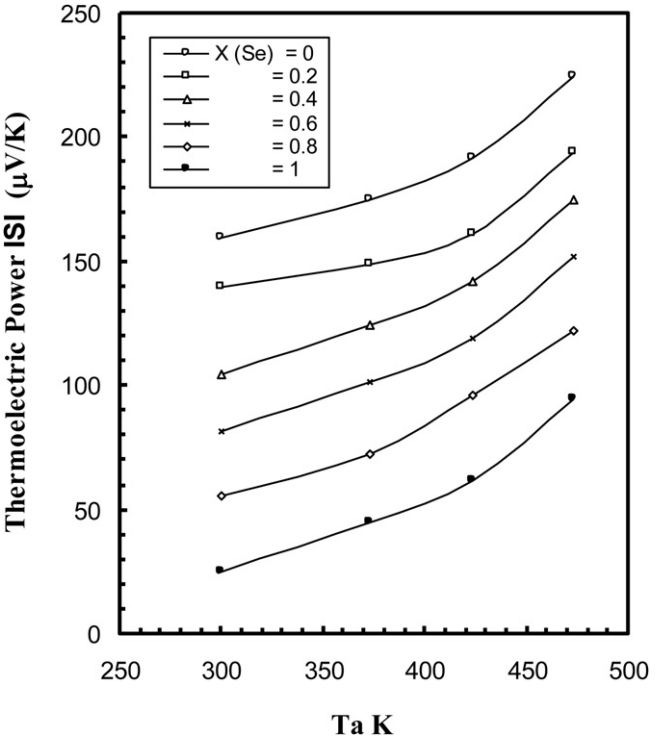

Fig. 6. Variation of thermoelectric power (S) with annealing temperature for the as-deposited (300 K) $Bi_2(Te_{1-x}Se_x)_3$ thin films.

the electrical conductivity and thermoelectric power using the relation: ($p = S^2\sigma$). We can see that, the calculated values of the power factor p for the samples under investigation are increased by increasing annealing temperature and decreased by increasing Se content. Therefore, it was confirmed that the annealing treatment is necessary for these materials to reduce the antistructure defects and to improve the thermoelectric properties.

3.4. Hall mobility

The Hall mobility μ_H of the investigated films was calculated from the relation: $\mu_H = R_H\sigma$ at different annealing temperatures.

Fig. 7 shows the log–log plot of Hall mobility μ_H versus the temperature T for the annealed films at 473 K, to deduce the power variation law of mobility ($\mu \propto T^a$), where the value of the exponent a depends on the scattering mechanism.

The theoretical value for acoustic phonon scattering leads to values of a which are close to 1.5 according to the law of mobility. The deviation from this law can be explained if we take into account the scattering by ionized impurities as an additional mechanism. This additional mechanism leads to a variation of mobility according to $T^{3/2}$.

For temperature higher than 400 K (400–500 K), the Hall mobility decreases linearly with temperature for the investigated samples as seen from Fig. 7. The calculated values of a in this temperature range are less than 3/2 indicating that the mobility is due to acoustic phonon scattering in addition to ionized impurity scattering mechanism [21,29,30]. We conclude that the most probable scattering mechanisms are the acoustic phonon scattering in addition to the ionized impurity scattering. The high carrier concentration obtained demonstrated that the number of ionized defects is not negligible in our samples.

3.5. Number of free carriers n

The carrier concentration was calculated from the relation; $n = 1/(eR_H)$. The plots of $\log(n)$ and the reciprocal of the absolute temperature of the investigated samples of different compositions annealed at 473 K are shown in Fig. 8. The number of free carriers (n) in the temperature interval from 300 to 400 K is constant indicating full ionization of the impurity centers, while for temperature greater than 400 K, the number of free carriers increases markedly as the temperature increases indicating the intrinsic conduction for all investigated samples. For temperature greater than 400 K, the number of free carriers varies exponentially with temperature meaning linear relation; the slope of these lines gives the energy gaps [24]. The calculated energy gaps are found to be in good agreement with those obtained from the electrical conductivity as listed in Table 2.

It is found also that, the carrier concentration n increases by increasing annealing temperature, while n decreases by increasing Se contents for all samples. This behaviour may be attributed to the difference of the electro-negativity and the atomic radii of both Se and Te atoms.

3.6. Effective mass

The effective mass (m^*/m_0) is one of the most important physical parameters and is related to the thermoelectric power, S, and the calculated carrier concentration, n, obtained from the Hall coefficient R_H by the relation [24]:

$$S = k/e\left\{C + \ln\left[2\left(2\pi m^* KT\right)^{3/2}\right]/h^3 n\right\} \quad (3)$$

where K is the Boltzmann's constant, e is the electronic charge, T is the absolute temperature, n is the carrier concentration, C is a constant depending on the type of scattering.

We found that m^*/m_0 decreases quadratically as x increases while it increases by increasing thermal annealing for all investigated samples as shown in Fig. 9.

However, as there is no reported data on the effective mass of these compositions, we cannot assure the value of m^* unless more detail work will be performed on these compositions.

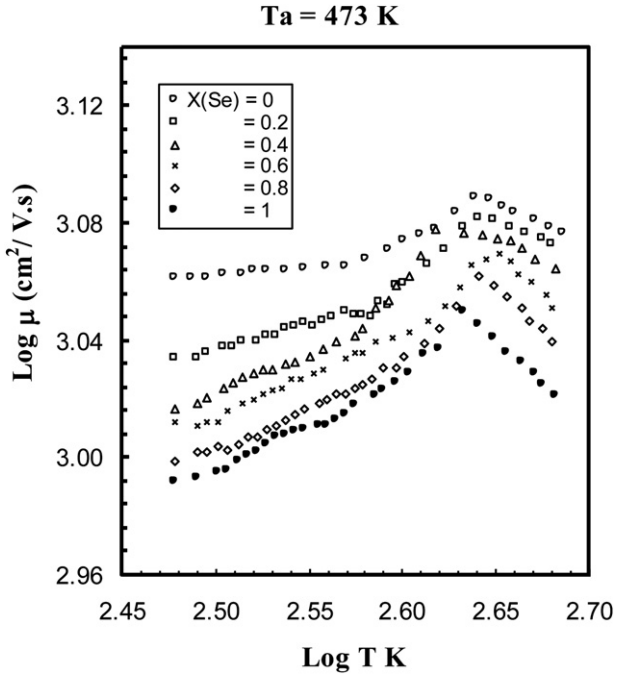

Fig. 7. Plots of log μ against log T for $Bi_2(Se_xTe_{1-x})_3$ thin films annealed at 473 K.

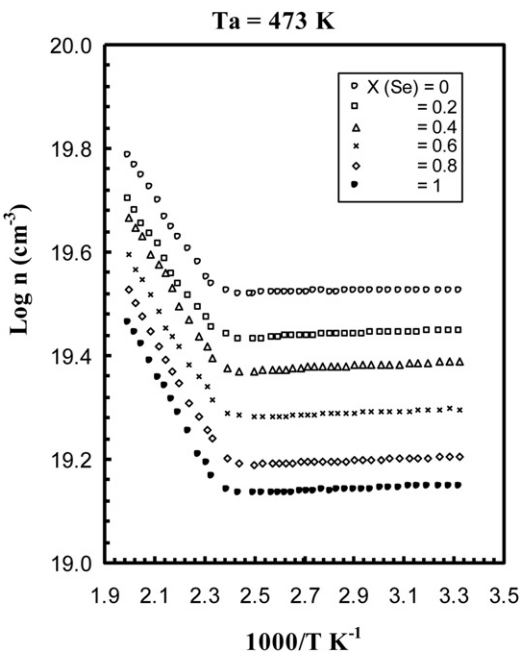

Fig. 8. Variation of free carrier density $\log(n)$ with reciprocal temperature ($1000/T$) for $Bi_2(Se_xTe_{1-x})_3$ thin films annealed at 473 K.

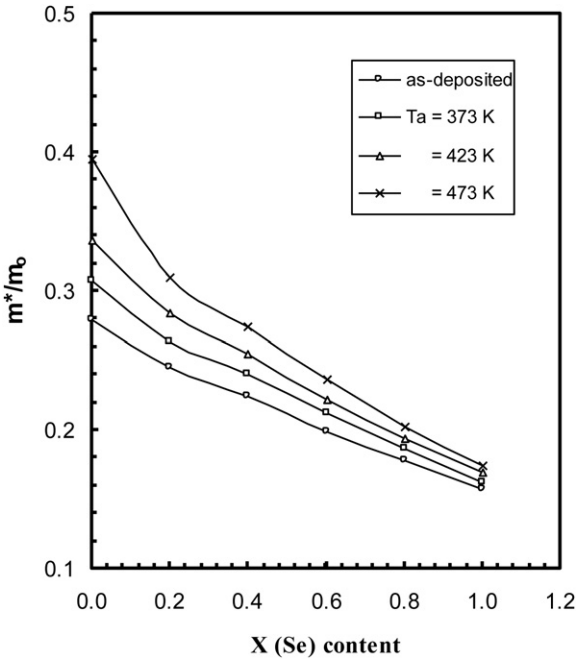

Fig. 9. Variation of effective mass (m^*/m_0) with composition for the as-deposited (300 K) and annealed $Bi_2(Te_{1-x}Se_x)_3$ thin films at $T_a = 373$, 423, 473 K.

3.7. Electronic thermal conductivity, K_{el}

The thermal conductivity (K) is the sum of the contributions due to the crystal lattice (K_{ph}) and electrons (K_{el}) [31]

$$K = K_{ph} + K_{el} \quad (4)$$

The lattice factor K_{ph} has a low value in polycrystalline alloy and is negligible with respect to K_{el}, according to the fact that the K_{ph} is inversely proportional to the mass of the unit cell [32] and the grain size [33]. However, the electronic K_{el} of K was calculated from the Wiedemann-Franz law [34]:

$$K_{el} = L\sigma T \quad (5)$$

where $L = 2.445 \times 10^{-8}\,W\Omega/K^2$ is Lorentz number [35], σ is the electrical conductivity and T is temperature.

Fig. 10 shows the compositional dependence of electronic thermal conductivity K_{el} for the as-deposited thin films and those annealed at different annealing temperatures. It appears that, K_{el} decreases sharply by increasing *Se* contents, while the electronics thermal conductivity K_{el} increases by increasing annealing temperature for all the investigated samples. These results are in good agreement with the electrical conductivity σ data as discussed before.

Similar results were observed for other workers [21,29,36] for composition $Bi_2(Te_{1-x}Se_x)_3$ single crystal with $x = 0$, $x = 1$ and $x < 0.15$, and a comparison for $x = 0.2$, 0.4, 0.6, 0.8 could not be made since there is no report on thermal conductivity K for these compositions.

3.8. Figure of merit

A selection criterion of the narrow band gap thermoelectric materials is given by the dimensionless figure of merit $ZT = (S^2\sigma/K)T$, where S is the Seebeck coefficient as thermoelectric power, σ is the electrical conductivity and K is the thermal conductivity and T is the absolute temperature.

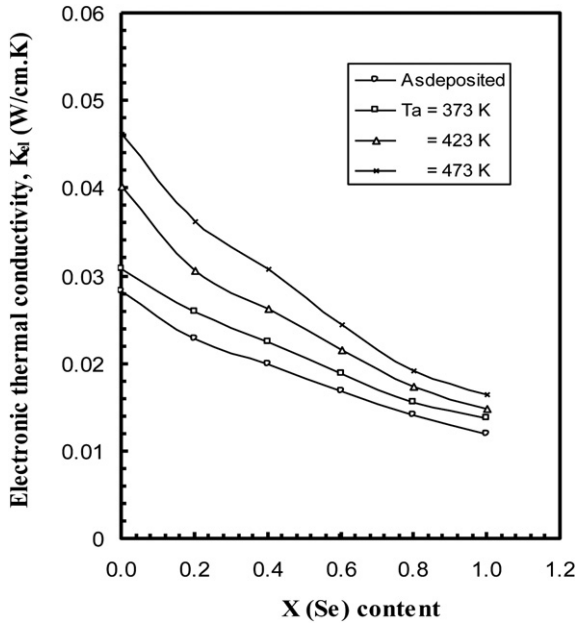

Fig. 10. Variation of electronic thermal conductivity with composition x for as-deposited (300 K) and annealed $Bi_2(Te_{1-x}Se_x)_3$ thin films at $T_a = 373$, 423, 473 K.

Plots of the calculated thermoelectric figure of merit ZT as a function of annealing temperature are shown in Fig. 11. It is evident that, ZT increases by increasing annealing temperature, while it decreases by increasing *Se* contents x for all investigated sample.

It is obvious that there is a strong correlation between the change in electrical conductivity σ before and after annealing and the rate of enhancement in ZT due to the annealing. That is the rate of enhancement in the ZT is due to increasing σ by annealing.

Recently, Yamashita et al. [37] studied the influence of annealing on the distribution of the figure of merit in $Bi_2Te_{2.8}2Se_{0.18}$ ingot and they observed that ZT increases after annealing of 2 h in vacuum.

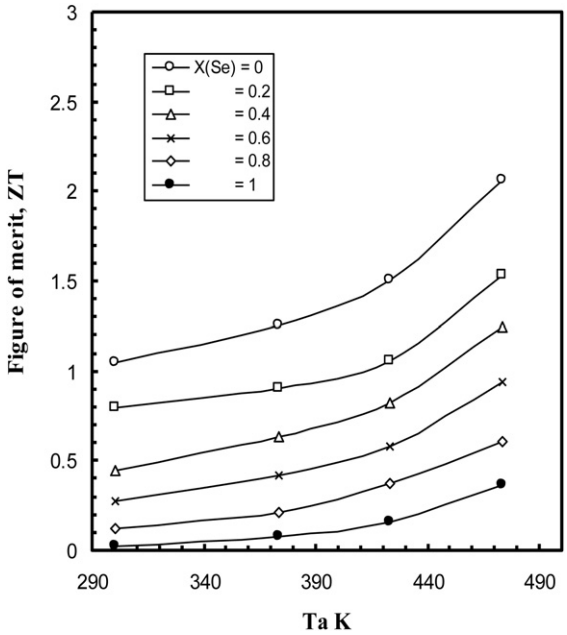

Fig. 11. Variation of figure of merit, ZT with annealing temperature $T_a = 373$, 423, 473 K for as-deposited (300 K) $Bi_2(Te_{1-x}Se_x)_3$ thin films.

These results agree well with our studies and also with other workers [21,29,36].

More detailed work will be performed on this composition to have the highest *ZT* value, by optimizing the annealing condition and the carrier concentration in the future.

4. Conclusion

Nearly stoichiometric Bi_2Te_3, $Bi_2Te_{2.4}Se_{0.6}$, $Bi_2Te_{1.8}Se_{1.2}$, $Bi_2Te_{1.2}Se_{1.8}$, $Bi_2Te_{0.6}Se_{2.4}$ and Bi_2Se_3 films were prepared by thermal evaporation of the synthesize bulk materials. The electrical resistivity, thermoelectric power, and Hall voltage were measured for films annealed at different annealing temperatures in the temperature range 300–500 K.

The analysis of the d.c. conductivity revealed degenerate semiconductor behaviour with the existence of two distinct thermal activation energies for each composition, ΔE_1 and ΔE_2 due to extrinsic and intrinsic conduction mechanisms in the temperature range 300–400 K and 400–500 K; respectively. However, the two activation energies ΔE_1 and ΔE_2 increase by increasing Se content and the energy gap was determined from the intrinsic region. The analysis of the thermoelectric power revealed the degenerate semiconductor behaviour with n-type conduction. From the determined value of Hall constant, R_H, for different compositions, Hall mobility, μ_H carrier concentration, n, effective mass, m^*/m_0, and thermal conductivity, K_{el}, were deduced showing compositional dependence.

One of the most interesting results of this study is the fact that, the introduction of Se into Bi_2Te_3 does not lead to an increase in the figure of merit *ZT*, while *ZT* is enhanced most significantly by the annealing of the low resistivity samples.

References

[1] Scherrer H, Chitroub M, Roche C, Scherrer S. Thermoelectric, ICT. In: Proceeding of international conference. Piscataway, NJ, USA: IEEE; 1998. p. 115–20.
[2] Kulbachinski VA, Kaminski AYu, Kindo K, Narumi Y, Sugak S, Kawazaki. Phys Status Solidi B 2002;22G(3):146.
[3] Slack GA. In: Rowe DM, editor. CRC hand book of thermoelectrics; 1995. p. 407.
[4] Dheepa J, Sathyamorthy R, Velumino S. Mater Character 2007;58:782.
[5] Snbramanian S, Pathinathan Padiy D. Mater Chem Phys 2008;107:392.
[6] Austin IG, Sheard AR. J Electron Control 1957;3:236.
[7] Greenaway DL, Harbeke G. J Phys Chem Solids 1965;26:1585.
[8] Slack GA. Thermoelectric materials – new directions and approaches. Mater Res Soc Symp Proc 1997;478:47.
[9] Hsu KF, Loo S, Guo F, Chen W, Dyck JS, Uher C, et al. Science 2000;303:818.
[10] Chung DY, Hogan T, Brazis, Rocci-Lane M, Kannewurf C, Bastea M, et al. Science 2000;287:1024.
[11] Disalvo FJ. Science 1999;285:703.
[12] Lyeo HK, Khajetoorians AA, Shi L, Pipe KP, Rajeev JR, Shakouri A, et al. Science 2004;303:816.
[13] Wang W, Huang Q, Jia FL, Zhu J. J Appl Phys 2004;96:615.
[14] Damodara V, Selvaraj S. J Appl Phys 1999;86:1518.
[15] Michel S, Stein N, Scheider M, Boulanger C, Lecuire JM. J Appl Electrochem 2003;33:23.
[16] Miyazaki Y, Kajitani T. J Cryst Growth 2001;229:542.
[17] Tittes K, Bund A, Plieth W, Bentien A, Paschen S, Plotner M, et al. J. Solid State Electrochem 2003;7:714.
[18] Vasilevskiy D, Sami A, Simard JM, Masut R. J Appl Phys 2002;92:2610.
[19] Coldsmid HJ. In: Proceeding of the fifth international conference on physical semiconductor; 1960. p. 1015.
[20] Kim D-H, Mitani T. J Alloys Compd 2005;399:14–9.
[21] Carle M, Pierrat P, Lahalle-Gravier C, Scherrer S, Scherrer H. J Phys Chem Solids 1995;56:201–9.
[22] Soliman LI, Nassary MM, Shaban HT, Salwa AS. Eur J Solids, in press.
[23] Tolansky S. In: Multiple-beam interference microscopy of metals. London: Academic Press; 1970. p. 55.
[24] Ioffe AF. Physics of semiconductors. London: Info. Search; 1960.
[25] Kumar Sushil, Hussain Muzammil, P.Sharma Thaneshwar, Husain Mushahid. J Phys Chem Solids 2003;64:367.
[26] Soliman LI, Nassary MM, Shaban HT, Salwa AS, in press.
[27] Kim T-S, Chun B-S. J Alloys Compd 2007;437:225–30.
[28] Saji A, Elizabeth M, Ampili S, .Yang S-Ho, Jeung Ku K. J Phys: Condens Matter 2005;17:2873–88.
[29] Saji A, Elizabeth M. Semicond Sci Technol 2003;18:745–54.
[30] Putly EH. The Hall effect and related phenomena. London: Butterworths; 1960. p. 146.
[31] Kim TS, Kim TK, Hong SJ, Chum BS. Mater Sci Eng B 2002;90(1):42–6.
[32] Kuznetsova LA, Kuznetsova VL, Row DM. J Phys Chem Solids 2000;61(8):169.
[33] Chen G, Zang T, Borca-Tasciue T, Song D. Mater Sci Eng A 2000;292 (2):155–61.
[34] Goldsmid HJ. Thermoelectric refrigeration. New York: Plenum; 1964.
[35] Phys Rev B 1970;1:1351–62.
[36] Vasilevskiy D, Sami A, Simard JM, Masut R. J Appl Phys 2002;92:2610.
[37] Yamashita Osamu, Tomiyoshi Shoichi. J Appl Phys 2004;95(11).